EUROPEAN ORGANIZATION FOR NUCLEAR RESEARCH

L3 Note 2568
July 4, 2000

Double Tag Events in Two Photon Collisions at LEP

The L3 Collaboration

Abstract

Double tag events in two photon collisions are studied using the L3 detector at the LEP center of mass energies $\sqrt{s} \simeq 189 - 202$ GeV. The cross-section of $\gamma^*\gamma^*$ collisions is measured at an average photon virtuality $\langle Q^2 \rangle = 15$ GeV^2. The results are in agreement with Monte Carlo predictions based on perturbative QCD, while the Quark Parton Model alone is insufficient to describe the data. The measurements are compared to LO and the NLO BFKL calculations.

Submitted to the
XXXth International Conference on High Energy Physics
July 27 - August 2, 2000, Osaka, Japan

1 Introduction

In this paper we present new results on double-tag two-photon events $e^+e^- \rightarrow e^+e^- hadrons$. The analysis for $\sqrt{s} \simeq 91$ GeV and $\sqrt{s} \simeq 183$ GeV was already published [1]. The data, collected at centre-of-mass energies $\sqrt{s} \simeq 189-202$ GeV, correspond to an integrated luminosity of 401 pb^{-1}. Both scattered electrons [1)] are detected in the small angle electromagnetic calorimeters. The virtuality of the two photons, Q_1^2 and Q_2^2, is in the range of 4 GeV^2 $< Q_{1,2}^2 <$ 40 GeV^2. The centre-of-mass energy of the two virtual photons, $\sqrt{\hat{s}} = W_{\gamma\gamma}$, ranges from 5 GeV to 90 GeV. Double-tag events have been measured in previous experiments [2] at lower values of Q^2 and $W_{\gamma\gamma}$.

The cross-section measurement of the two virtual photons is considered as "golden" process to test the BFKL dynamics which is proposed in [3]. For this scheme the $\gamma^*\gamma^*$ interaction can be seen as the interaction of two $q\bar{q}$ pairs scattering off each other via multiple gluon exchange. In the leading order approximation, the cross-section at the saddle point approximation for the collision of two virtual photons is [4, 5]:

$$\sigma_{\gamma^*\gamma^*} = \frac{\sigma_0}{\sqrt{Q_1^2 Q_2^2 Y}} \left(\frac{s}{s_0}\right)^{\alpha_P - 1} \approx \frac{\sigma_0}{\sqrt{Q_1^2 Q_2^2 Y}} \left(\frac{\hat{s}}{\sqrt{Q_1^2 Q_2^2}}\right)^{\alpha_P - 1} . \tag{1}$$

Here

$$\begin{aligned} \sigma_0 &= \text{const} \\ s_0 &= \frac{K\sqrt{Q_1^2 Q_2^2}}{y_1 y_2} \quad , \quad Y = \ln\left(s/s_0\right) \\ y_i &= 1 - (E_i/E_b)\cos^2(\theta_i/2) \end{aligned} \tag{2}$$

where E_b is the beam energy, E_i and θ_i are the energy and polar angle of the scattered electrons and α_P is the "hard Pomeron" intercept; K is a scale factor which accounts for higher order corrections. The centre-of-mass energy of the two-photon system is related to the e^+e^- centre-of-mass energy s by $\hat{s} = W_{\gamma\gamma}^2 \approx s y_1 y_2$. In leading order $(\alpha_P - 1) = (4\ln 2) N_c \alpha_s/\pi$, where N_c is the number of colours. Using $N_c = 3$ and $\alpha_s = 0.2$, $(\alpha_P - 1) \simeq 0.53$. Recently, effort has been devoted to improve the exact leading order calculation [3] by studying the effect of charm mass, of the variation of strong coupling constant α_s and the contribution of longitudinal photon polarization states [6]. Still these effects are not sufficient to describe our previous measurement [1]. One needs next to leading order corrections. It turns out that the NLO corrections [7] to the intercept "$\alpha_P - 1$" are negative for $\alpha_s > 0.16$. Different techniques [8–14] have been proposed to improve the NLO calculations in a suitable renormalization scheme thus giving values of $(\alpha_P - 1)$ in the range 0.17−0.33.

2 Monte Carlo Generators

Two different Monte Carlo generators PHOJET [15] and TWOGAM [16] are used to simulate double-tag two photon events. Both give a good description of the single-tag events [17] and use the GRV-LO [18] parton density in the photon to generate QCD processes.

[1)] Electron stands for electron or positron throughout this paper.

PHOJET is an event generator for pp, γp and quasi-real two-photon interactions, described within the Dual Parton Model. A transverse momentum cutoff, $p_t^{cut} = 2.5$ GeV, is applied to the partons of the resolved photons to separate soft from hard processes [19]. The complete electron-photon vertex for transversely polarized photons is simulated. PHOJET gives also a good description of the untagged $\gamma\gamma \rightarrow$ hadrons events [20].

TWOGAM generates three different processes separately in γp interactions: the Quark Parton Model, the QCD resolved photon contribution and the Vector Dominance Model (VDM). It uses LO matrix elements to describe the QCD single and double resolved photon interactions. A p_t^{cut} cut-off of the order of 3.5 GeV is applied in order to limit the use of LO formulae to the region of sufficiently 'hard' interactions.

The QPM cross-section $\mathrm{e^+e^-} \rightarrow \mathrm{e^+e^-q\bar{q}}$ is estimated with GALUGA [21][2)]. This Monte Carlo program provides the numerical computation of two-photon processes in $\mathrm{e^+e^-}$ collisions over the whole range of photon virtualities and the two-photon invariant mass $W_{\gamma\gamma}$. It contains all the photon polarization terms including interference terms corresponding to transverse and longitudinal helicity states of the photon. Thus it is useful to investigate the individual contributions to the differential cross-section. This program is also used to calculate two-photon luminosity.

The dominant backgrounds are $\mathrm{e^+e^-} \rightarrow \mathrm{e^+e^-}\tau^+\tau^-$, simulated by JAMVG [22], and single-tag two-photon hadronic events, where a hadron is misidentified as a scattered electron. The contamination by annihilation processes is simulated by PYTHIA [23] ($\mathrm{e^+e^-} \rightarrow$ hadrons), KORALZ [24] ($\mathrm{e^+e^-} \rightarrow \tau^+\tau^-$) and KORALW [25] ($\mathrm{e^+e^-} \rightarrow \mathrm{W^+W^-}$).

All Monte Carlo events are passed through a full detector simulation of the L3 detector [26, 27] using the GEANT [28] and the GEISHA [29] programs and are reconstructed in the same way as the data.

3 Data Analysis

3.1 Event Selection

The double-tag two-photon hadronic events are mainly triggered by two independent triggers: the central track [30, 31] and the single and double tag energy [32] triggers. The central track trigger requires at least two charged particles, each with $p_t > 150$ MeV, back-to-back in the transverse plane. The single$-$tag energy trigger requires an high energy cluster in one of the small angle electromagnetic calorimeters, in coincidence with at least one track in the central tracking chamber. For the double$-$tag trigger the back-to-back small angle electromagnetic calorimeters must each have a high energy cluster and no coincidence with the central detector is required. The total trigger inefficiency of the selected events is less than 1%.

Two-photon hadronic event candidates, $\mathrm{e^+e^-} \rightarrow \mathrm{e^+e^-}$hadrons, are selected using the following cuts:

- There must be two identified electrons, forward and backward (double-tag), in the small angle electromagnetic calorimeters. Each electron is identified as the highest energy cluster in one of the calorimeters, with energy greater than 40 GeV. The polar angle of the two tagged electrons has to be in the range 30 mrad $< \theta_1 <$ 66 mrad and 30 mrad $< \pi - \theta_2 <$ 66 mrad.

[2)] For comparison we have checked the QPM calculation in GALUGA with JAMVG [22]. The agreement is excellent.

- The number of particles, defined as tracks and isolated calorimeter clusters in the polar angle region $20° < \theta < 160°$, must be greater than 5. The tracks are selected by requiring a transverse momentum, p_t, greater than 100 MeV and a distance of closest approach in the transverse plane to the interaction vertex smaller than 10 mm. Isolated energy clusters are required to have transverse energy greater than 100 MeV and no nearby track inside a cone of 35 mrad half angle. These cuts are illustrated in Fig 1. One can see that the double−tag data is well reproduced by the PHOJET and TWOGAM Monte Carlos.
- The value of $Y = \ln(s/s_0)$ is required to be in the range $2 \leq Y \leq 7$.
- The opening angle between the scattered electrons must be smaller than 179.5°, to reject Bhabha events.

After these cuts, 336 events are selected with an estimated background of 31 events from misidentified single-tag and 21 events from $e^+e^- \rightarrow e^+e^-\tau^+\tau^-$. The contamination from annihilation processes (4 events) is negligible.

Figure 2 shows the kinematic distributions of E_{tag}/E_{beam}, Q^2, θ_{tag} and of the ratio $\log(Q_1^2/Q_2^2)$ of the scattered electrons. PHOJET and TWOGAM Monte Carlos describe the data reasonably well. The Monte Carlo distribution shown are normalized to the number of data events.

In Fig. 3, the distributions of $W_{\gamma\gamma}$ and Y are presented. The variable $W_{\gamma\gamma}$ is calculated from the four-vector of the two scattered electrons, taking advantage of the good resolution of their energy measurement (about 1.3% [27]). The $W_{\gamma\gamma}$ resolution is about 18% at $W_{\gamma\gamma}/\sqrt{s} = 0.08$ and about 6% at $W_{\gamma\gamma}/\sqrt{s} = 0.2$. Both PHOJET and TWOGAM give a reasonable description of the shape of the data. The absolute normalisation of PHOJET is about 18% too low. This difference can be due to high p_t^{cut} threshold which suppresses the charm production and to non-inclusion of longitudinal polarization of the two virtual photons in PHOJET.

Contrary to the case of untagged or single-tag events the $W_{\gamma\gamma}$ measurement does not rely on the W_{vis} measurement of invariant mass of hadronic final state. Figure 4 shows a good correlation of $W_{\gamma\gamma}$ generated versus $W_{\gamma\gamma}$ reconstructed. The analysis is, therefore, less dependent on Monte Carlo modelling.

3.2 Double-tag cross-section

The cross-sections are measured in the kinematic region:

- $E_{1,2} > 30$ GeV, 30 mrad $< \theta_1 <$ 66 mrad and 30 mrad $< \pi - \theta_2 <$ 66 mrad.
- $2 \leq Y \leq 7$.

The data are corrected for efficiency and acceptance with PHOJET. The correction factors vary from 47% to 96% as a function of Y. The correction factors calculated with TWOGAM are similar. Figure 5 shows the correction factors as a function of the variable Y computed with PHOJET. The differential cross-sections $\mathrm{d}\sigma(e^+e^- \rightarrow e^+e^- hadrons)/\mathrm{d}Y$ are measured in four ΔY intervals and are listed in Table 1.

The systematic error due to the selection cuts is 5%, estimated by varying the cuts on energy of the scattered electron, the variable Y and the number of particles. The uncertainty on the cross-section from the background estimation of single-tag events is 4%. The uncertainty due to the acceptance correction is 5%, estimated by comparing PHOJET and TWOGAM. The different systematic uncertainties are added in quadrature to give the total systematic uncertainties listed in Table 1.

As can be seen in Table 1 and in Fig. 6a) and b), the data are in agreement with the predictions of the QCD Monte Carlo model implemented in PHOJET and TWOGAM. The QPM cross-section is not sufficient to describe the data. The value of the cross section at $5 < Y < 7$ exceeds the Monte Carlo prediction by about 3.5 standard deviations.

From the measurement of the $e^+e^- \to e^+e^- hadrons$ cross-section, σ_{ee}, we extract the two-photon cross-section, $\sigma_{\gamma^*\gamma^*}$, by using only the transverse photon luminosity function [21, 33], $\sigma_{ee} = L_{TT} \cdot \sigma_{\gamma^*\gamma^*}$. We measure an effective cross-section containing contributions from transverse (T) and longitudinal (L) photon polarizations:

$$\sigma_{\gamma^*\gamma^*} = \sigma_{TT} + \epsilon_1\sigma_{TL} + \epsilon_2\sigma_{LT} + \epsilon_1\epsilon_2\sigma_{LL} \qquad \epsilon_i = \frac{L_L}{L_T} = \frac{2(1-y_i)}{1+(1-y_i)^2} \tag{3}$$

where ϵ_i is the ratio of longitudinal and transverse photon luminosity functions. In the present kinematical region the average value of ϵ_i is 0.95, but the values of σ_{TL}, σ_{LT} and σ_{LL} were expected to be small [4]. The distributions of the coefficient ϵ and the variable y are shown in figure 7 and compared to Monte Carlo predictions. Recently, studies were performed to include the longitudinal photon polarization states [6]. The sum of all the polarization terms increases the exact LO cross section by more than 40% compared to the transverse contribution alone.

In Figure 8a) we show $\sigma_{\gamma^*\gamma^*}$, after subtraction of the full QPM contribution given in Table 2, as a function of Y. Using an average value of Q^2, $\langle Q^2\rangle = 15$ GeV^2, we calculate the one-gluon exchange contribution with the asymptotic formula (Eq. 10.2 of Ref. [4]). The expectations are below the data. The leading order expectations of the BFKL model (Eq. 4.19 of Ref. [4]), shown as a dotted line in figure 8a), are too high. By leaving α_P as a free parameter and $K = 1$, a fit of equation 1 to the data, yields:

$$\alpha_P - 1 = 0.36 \pm 0.02 \quad \text{with } \chi^2/\text{d.o.f} = 0.98/3 \tag{4}$$

If the energy scale factor K is a free parameter and $(\alpha_P - 1)$=0.53, the fit to the data yields:

$$K = 6.4 \pm 1.0 \quad \text{with } \chi^2/\text{d.o.f} = 1.34/3\ . \tag{5}$$

These results are shown in figure 8b) as a continuous and dotted lines respectively. The value of $(\alpha_P - 1)$, smaller than expected from the LO BFKL calculation at the saddle point approximation, and the scale factor K much larger than unity indicate that higher order corrections are important.

Figure 9 in top shows the comparison of the exact LO BFKL calculation including the longitudinal photon polarization states, the charm mass efffect and the variation of strong coupling constant α_s [6] with the LO BFKL calculation at saddle point approximation [4, 5]. Also shown (bottom)are the different photon polarization terms contributing to the exact LO BFKL calculation. Clearly the LO predictions are higher than the data. NLO calculations are in progress [9, 13, 14] which agree better with the experimental results.

4 Conclusions

The cross-sections of double-tag $e^+e^- \to e^+e^- hadrons$ events is measured at $\sqrt{s} \simeq 189-202$ GeV. The events are described by the PHOJET and TWOGAM Monte Carlo model which use the GRV-LO parton density in the photon and leading order perturbative QCD. The two-photon cross-sections are higher than the QPM and one-gluon exchange expectations but lower than the LO BFKL predictions. NLO BFKL calculations are necessary to expalin these results.

Acknowledgements

We express our gratitude to the CERN accelerator divisions for the excellent performance of the LEP machine. We acknowledge with appreciation the effort of all engineers, technicians and support staff who have participated in the construction and maintenance of this experiment.

References

[1] L3 Collab., M. Acciarri et al., Phys. Lett. B 453 (1999) 333-341.

[2] PLUTO Coll., C. Berger *et al.*, Phys. Lett. **B 142** (1984) 119;
TPC/2γ Coll., D. Bintinger *et al.*, Phys. Rev. Lett. **54** (1985) 763;
MD-1 Coll., S.E. Baru *et al.*, Z. Phys. **C 53** (1992) 219;
TOPAZ Coll., R. Enomoto *et al.*, Phys. Lett. **B 368** (1996) 299.

[3] E.A. Kuraev, L.N. Lipatov and V.S. Fadin, Sov. Phys. JETP **45** (1977) 199;
Ya.Ya. Balitski and L.N. Lipatov, Sov. J. Nucl. Phys. **28** (1978) 822.

[4] S.J. Brodsky, F. Hautmann and D.E. Soper, Phys. Rev. **D 56** (1997) 6957.

[5] J. Bartels, A. De Roeck and H. Lotter, Phys. Lett. **B 389** (1996) 742;
J. Bartels, A. De Roeck, C. Ewerz and H. Lotter, hep-ph/9710500.

[6] J. Bartels, C. Ewerz, R. Staritzbichler, hep-ph/0004029.

[7] V. S. Fadin and L. N. Lipatov, Phys. Lett. **B 429** (1998) 127;
G. Camici and M. Ciafaloni, Phys. Lett. **B 430** (1998) 349
and references therein.

[8] V. S. Fadin and L. N. Lipatov, Proc. Theory Institute on Deep Inelastic Diffraction, ANL, Argonne, September 14 - 16, 1998;
C. R. Schmidt, Phys. Rev. **D 60** (1999) 074003;
J. R. Forshaw, D. A. Ross and A. Sabio Vera, Phys. Lett. **B 455** (1999) 273;
S.J. Brodsky *et al.*JETP Lett. **70** (1999) 15, hep-ph/99101229.

[9] G. Salam, JHEP **9807** (1998) 019.

[10] M. Ciafaloni, D. Colferai and G. P. Salam, Phys. Rev. **D 60** (1999) 114036;
M. Ciafaloni and D. Colferai, Phys. Lett. **B 452** (1999) 372.

[11] R. S. Thorne, Phys. Rev. **D 60** (1999) 054031.

[12] G. Altarelli, R. D. Ball and S. Forte, CERN-TH/2000-010 (2000), hep-ph/0001157.

[13] V. T. Kim, L. N. Lipatov and G. B. Pivovarov, hep-ph/9911228 and hep-ph/9911242;
V. Kim, private communication.

[14] N.N. Nikolaev,J. Speth and V.R. Zoller, hep-ph/0001120.

[15] PHOJET version 1.05c is used.
R. Engel, Z. Phys. **C 66** (1995) 203;
R. Engel and J. Ranft, Phys. Rev. **D 54** (1996) 4244.

[16] TWOGAM version 2.03 is used.
L. Lönnblad *et al.*, "$\gamma\gamma$ event generators", in Physics at LEP2, ed. G. Altarelli, T. Sjöstrand and F. Zwirner, CERN 96-01 (1996), Volume 2, 224.
S. Nova *et al.*, DELPHI Note 90-35 (1990).
We thank our colleagues from DELPHI to make their program available to us.

[17] L3 Coll., M. Acciarri *et al.*, Phys. Lett. **B 436** (1998) 403;
L3 Coll., M. Acciarri *et al.*, Phys. Lett. **B 447**) (1999) 147.

[18] M. Glück, E. Reya and A. Vogt, Phys. Rev. **D 45** (1992) 3986;
M. Glück, E. Reya and A. Vogt, Phys. Rev. **D 46** (1992) 1973.

[19] J.H. Field, F. Kapusta and L. Poggioli, Phys. Lett. **B 181** (1986) 362;
J.H. Field, F. Kapusta and L. Poggioli, Z. Phys. **C 36** (1987) 121.

[20] L3 Coll., M. Acciarri *et al.*, Phys. Lett. **B 408** (1997) 450.

[21] G.A. Schuler, Comput. Phys. Commun. **108** (1998) 279.

[22] J.A.M. Vermaseren, Nucl. Phys. **B 229** (1983) 347.

[23] T. Sjöstrand, Comp. Phys. Comm. **82** (1994) 74.

[24] S. Jadach, B.F.L. Ward and Z. Wąs, Comp. Phys. Comm. **79** (1994) 503.

[25] M. Skrzypek, S. Jadach, W. Placzek and Z. Wąs, Comp. Phys. Comm. **94** (1996) 216;
M. Skrzypek, S. Jadach, M. Martinez, W. Placzek and Z. Wąs, Phys. Lett. **B 372** (1996) 289.

[26] L3 Collab., B. Adeva *et al.*, Nucl. Inst. Meth. **A 289** (1990) 35; M. Acciarri *et al.*, Nucl. Inst. Meth. **A 351** (1994) 300; M. Chemarin *et al.*, Nucl. Inst. Meth. **A 349** (1994) 345; A. Adam *et al.*, Nucl. Inst. Meth. **A 383** (1996) 342.

[27] I.C. Brock *et al.*, Nucl. Inst. Meth. **A 381** (1996) 236.

[28] R. Brun *et al.*, GEANT 3.15 preprint CERN DD/EE/84-1 (Revised 1987).

[29] H. Fesefeldt, RWTH Aachen report PITHA 85/2 (1985).

[30] P. Béné *et al.*, Nucl. Inst. Meth. **A 306** (1991) 150.

[31] D. Haas *et al.*, Nucl. Inst. Meth. **A 420** (1999) 101.

[32] R. Bizzarri *et al.*, Nucl. Inst. Meth. **A 283** (1989) 799.

[33] V.M. Budnev *et al.*, Phys. Rep. **C 15** (1975) 181.

189 − 202 GeV			
ΔY	DATA $d\sigma/dY$(pb)	PHOJET $d\sigma/dY$ (pb)	QPM $d\sigma/dY$ (pb)
$2.0-2.5$	$0.50 \pm 0.07 \pm 0.03$	0.40	0.32
$2.5-3.5$	$0.29 \pm 0.03 \pm 0.02$	0.29	0.17
$3.5-5.0$	$0.15 \pm 0.02 \pm 0.01$	0.14	0.05
$5.0-7.0$	$0.08 \pm 0.01 \pm 0.01$	0.03	0.006

Table 1: The differential cross-section, $d\sigma(e^+e^- \to e^+e^- hadrons)/dY$ measured in the kinematic region defined in the text, at $\sqrt{s} \simeq 189-202$ GeV. The first error is statistical and the second is systematic. The predictions of PHOJET and of the QPM are also listed.

ΔY	$\sigma^{TOT}_{\gamma^*\gamma^*}$ (nb)	$\sigma^{TOT-QPM}_{\gamma^*\gamma^*}$ (nb)
$2.0-2.5$	$8.51 \pm 1.23 \pm 0.57$	$2.98 \pm 1.23 \pm 0.57$
$2.5-3.5$	$7.20 \pm 0.79 \pm 0.48$	$3.01 \pm 0.79 \pm 0.48$
$3.5-5.0$	$6.48 \pm 0.76 \pm 0.43$	$4.34 \pm 0.76 \pm 0.43$
$5.0-7.0$	$9.46 \pm 1.76 \pm 0.63$	$8.67 \pm 1.76 \pm 0.63$

Table 2: The two-photon cross-section, $\sigma_{\gamma^*\gamma^*}$ without and after subtraction of the full QPM contribution, as a function of Y at $\sqrt{s} \simeq 189-202$ GeV. The first error is statistical and the second is systematic.

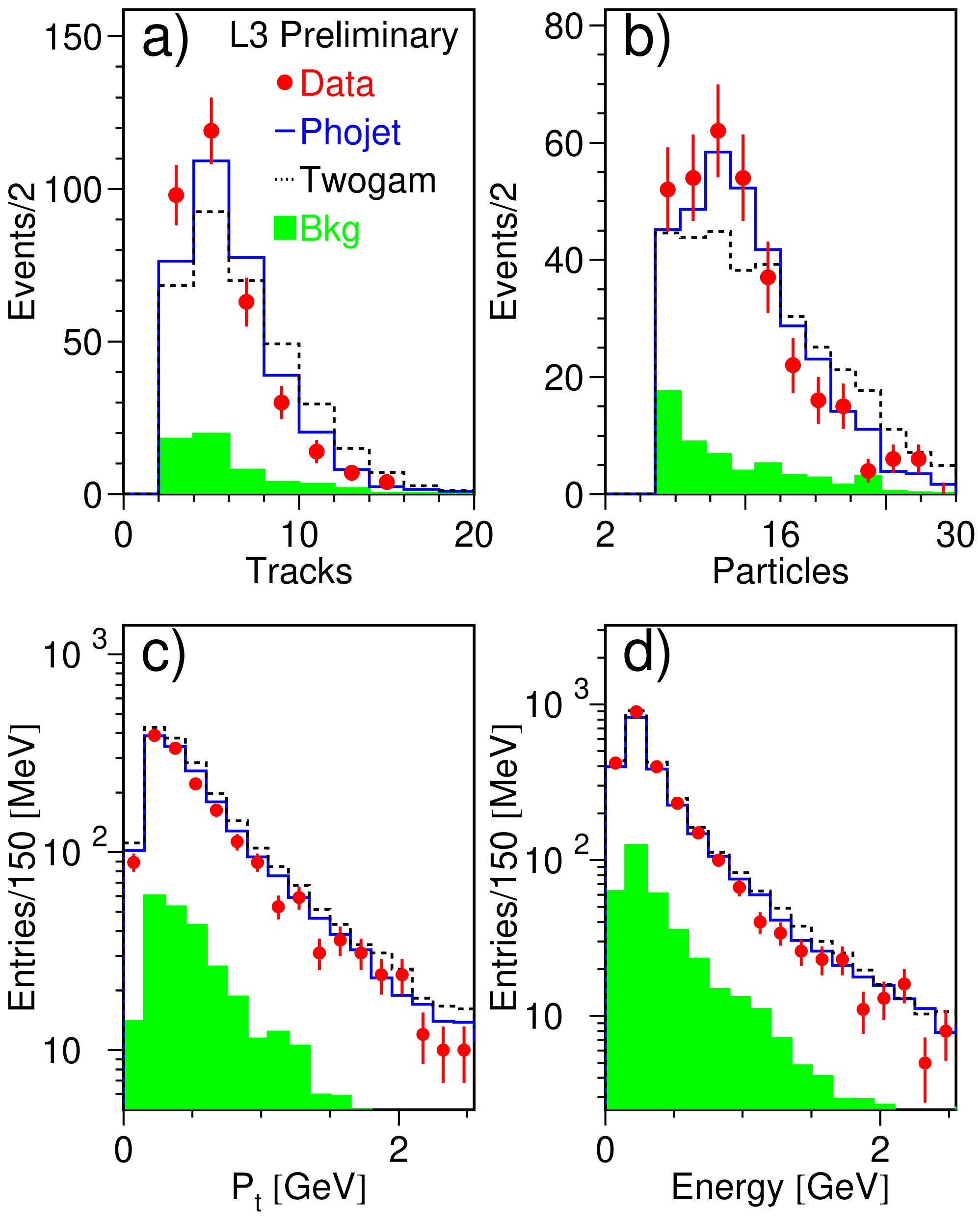

Figure 1: Distributions of a) Number of tracks, b) Number of particles, c) transverse momentum of tracks and d) energy of isolated calorimetric clusters. The data are compared to PHOJET and TWOGAM predictions, normalized to the total number of events in the data.

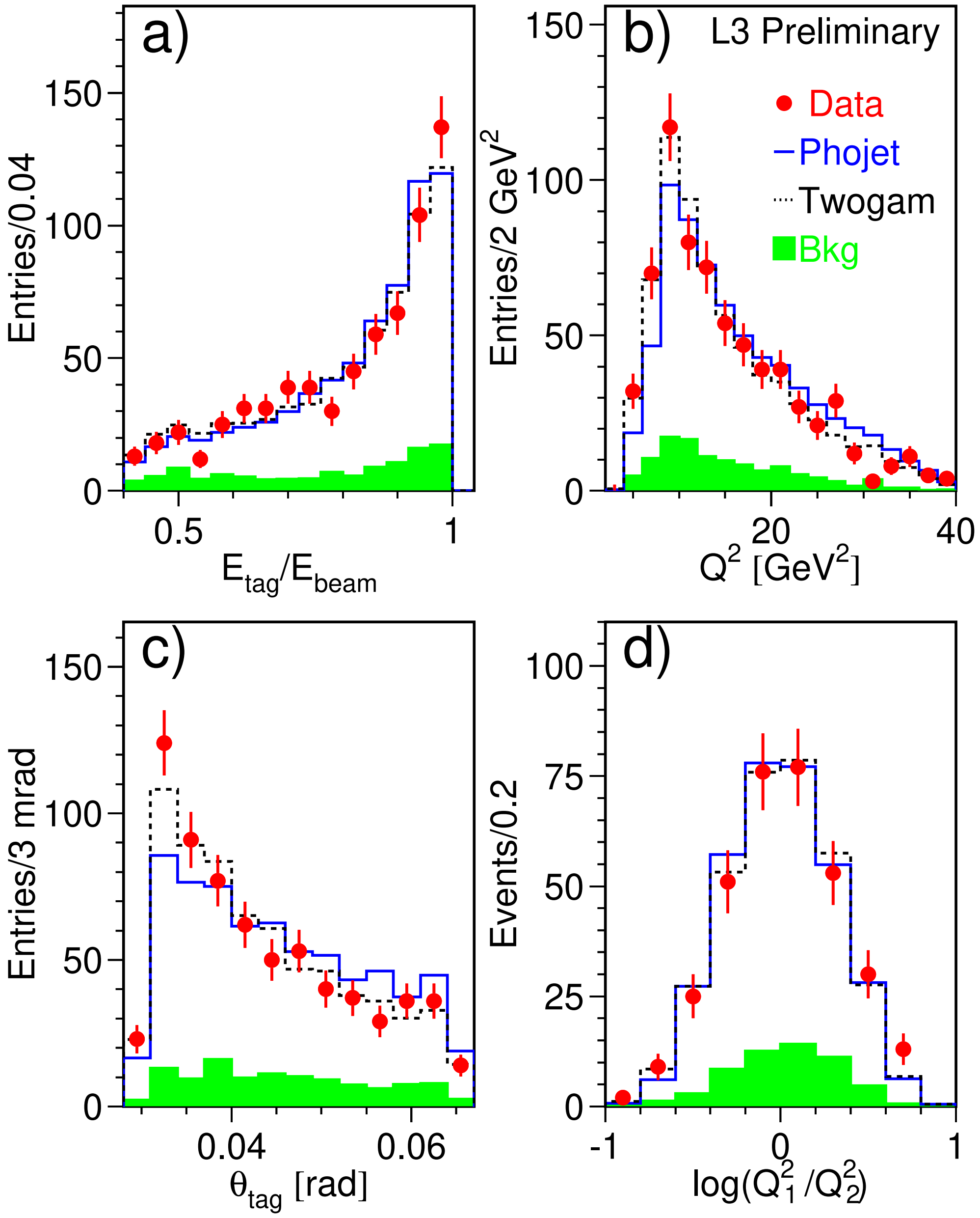

Figure 2: Distributions of a) E_{tag}/E_{Beam}, the energy of a tagging electron to the beam energy, b) Q^2 , c) θ_{tag} and d) the ratio Q_1^2/Q_2^2 of the scattered electrons. The data are compared to the Monte Carlo predictions, scaled to the number of data events.The backgrounds are mainly due to $e^+e^- \to e^+e^-\tau^+\tau^-$ and single tag two-photon hadronic events.

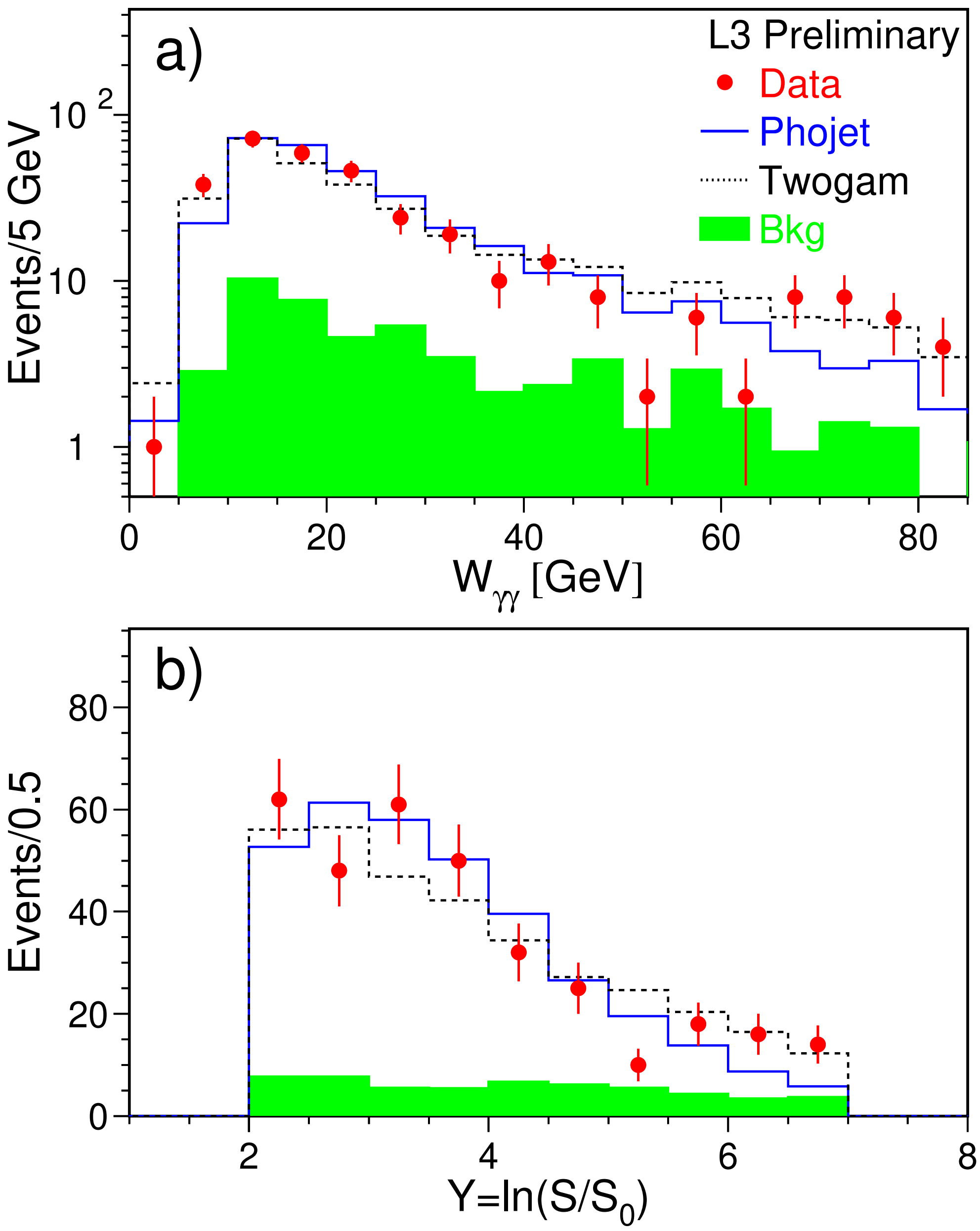

Figure 3: Distributions of a) the two-photon mass, $W_{\gamma\gamma}$, and b) the variable Y. The data are compared to the Monte Carlo predictions, normalised to the number of data events.

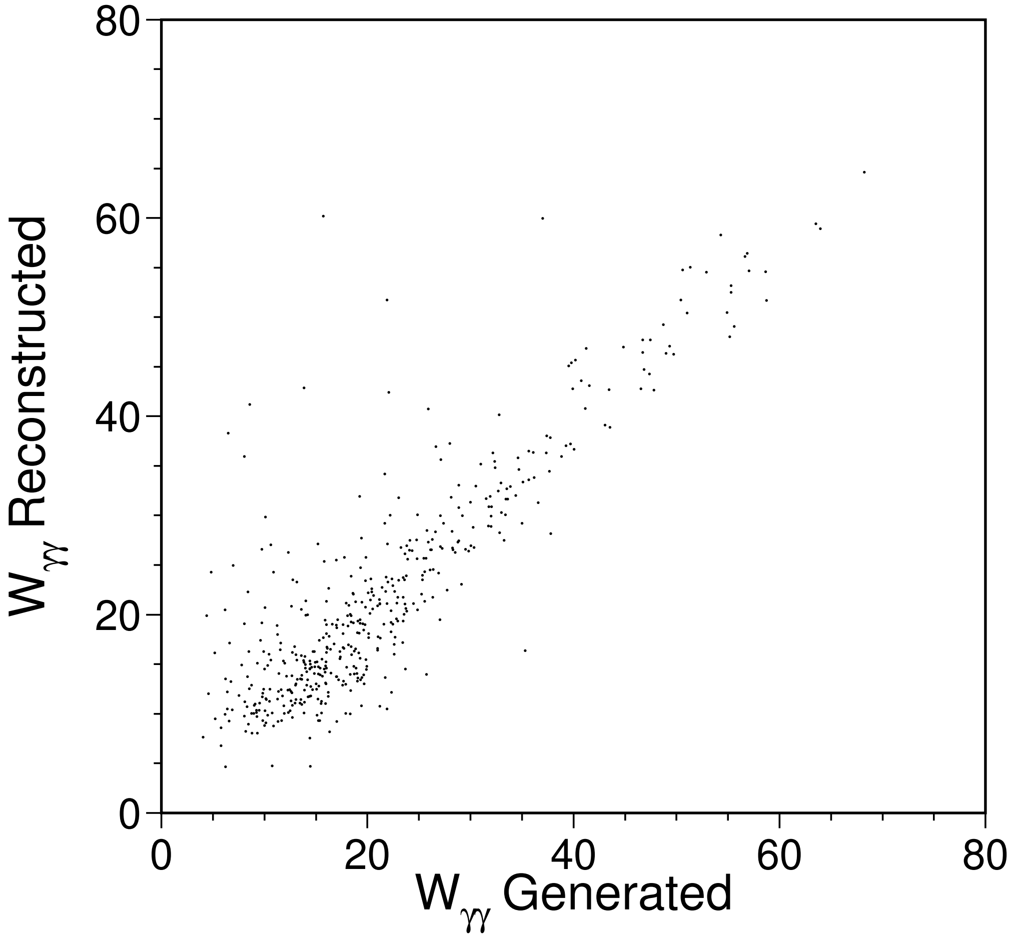

Figure 4: Distributions of the $W_{\gamma\gamma}$ reconstructed from the two scattered electron versus the $W_{\gamma\gamma}$ generated.

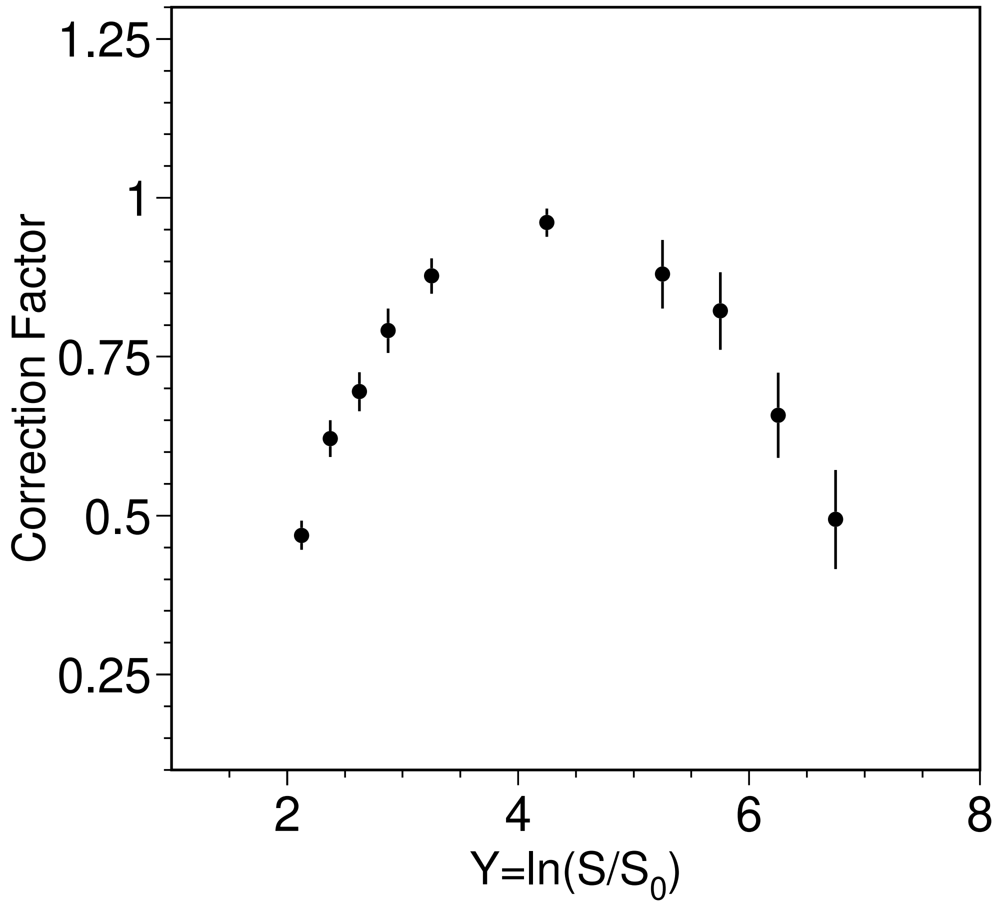

Figure 5: Correction factors as a function of the variable Y computed with PHOJET Monte Carlo.

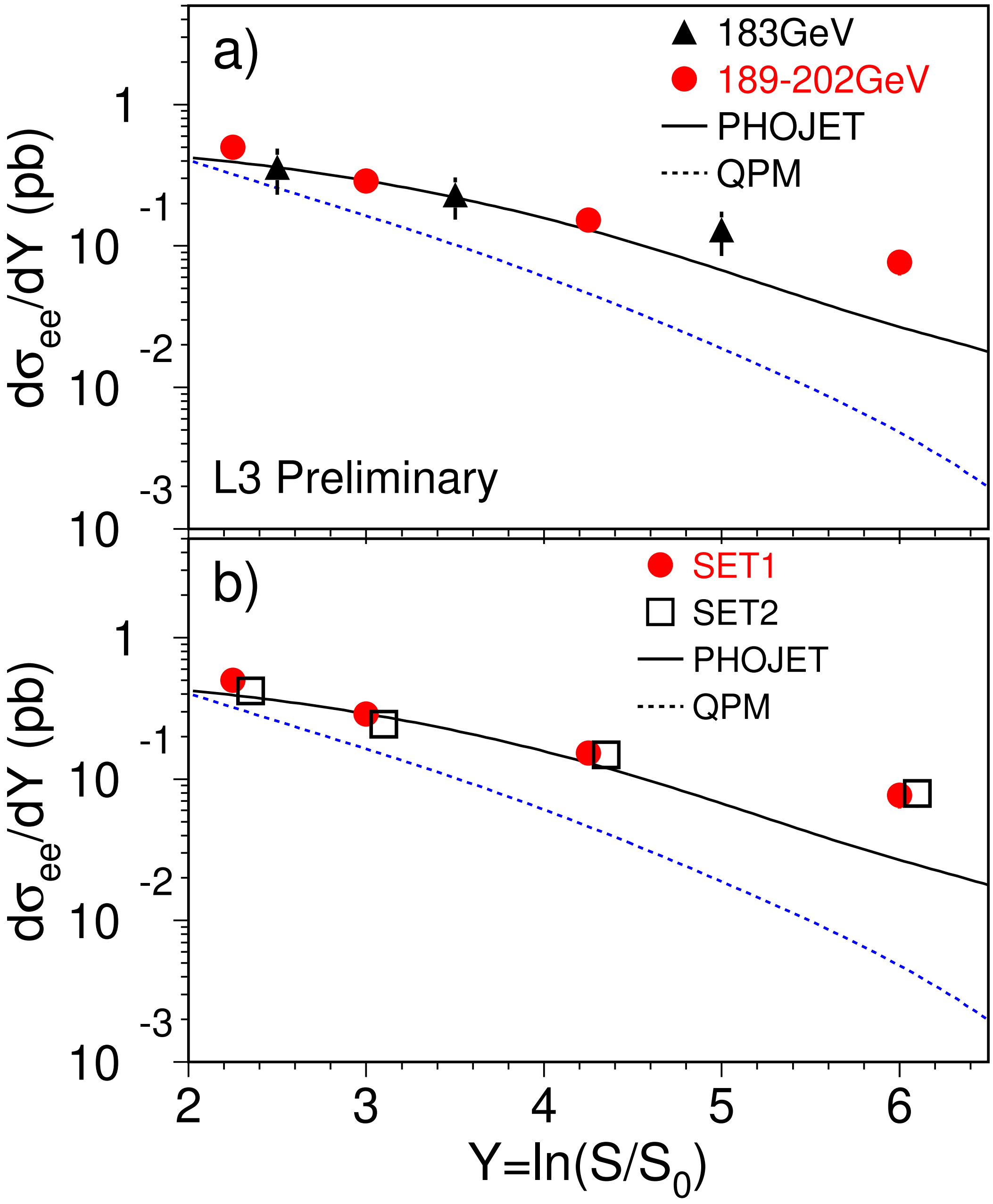

Figure 6: a) The cross-section of $e^+e^- \to e^+e^- hadrons$ as a function of Y in the kinematical region defined in the text at $\sqrt{s} \simeq 189-202$ GeV compared to our previous results $\sqrt{s} \simeq 183$ GeV. b) Comparison of the measured cross-sections corrected for acceptance using PHOJET(SET1) or TWOGAM(SET2). SET2 is shifted for better visibility. In both figures the predictions of PHOJET (continous line) and of the QPM model GALUGA(dashed line) are indicated.

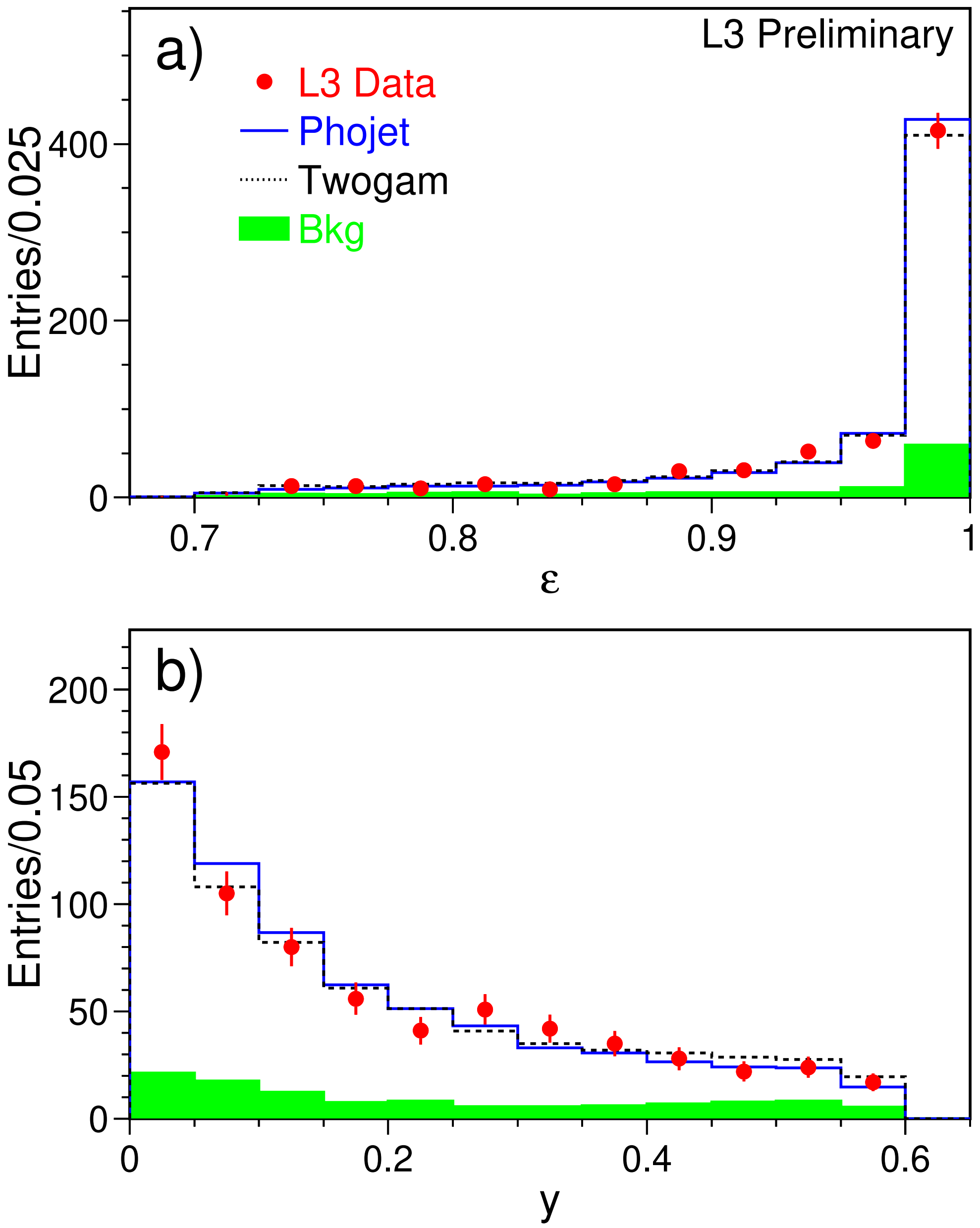

Figure 7: The distributions of a) the coefficient ϵ and b) the variable y as defined in the text (equation 4) compared to the predictions of the Monte Carlo models.

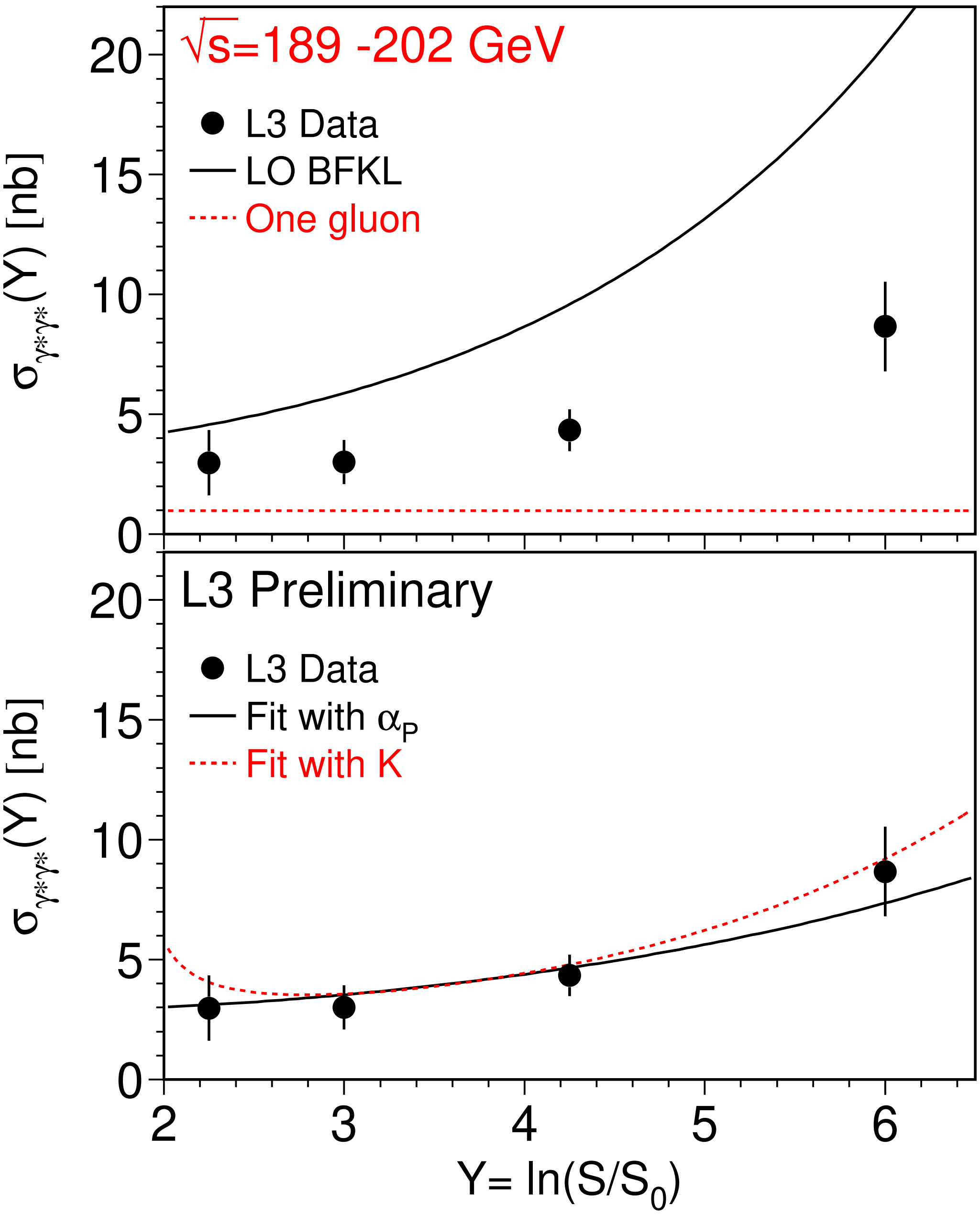

Figure 8: Two-photon cross-sections, $\sigma_{\gamma^*\gamma^*}$, after the subtraction of the QPM contribution at $\sqrt{s} \simeq 189 - 202$ GeV ($\langle Q^2 \rangle = 15$ GeV^2). (top) The data are compared to the predictions of the LO BFKL calculation at saddle point approximation(eq.1)(solid line) with K=1 and $(\alpha_P - 1) = 0.53$ and of the one-gluon exchange diagram (dashed line). (bottom) The solid line is the fit to the data of the LO BFKL (eq.1) with K=1 and the coefficient $(\alpha_P - 1)$ as a free parameter. The dashed line is the fit with $(\alpha_P - 1) = 0.53$ and the scale factor K as a free parameter.

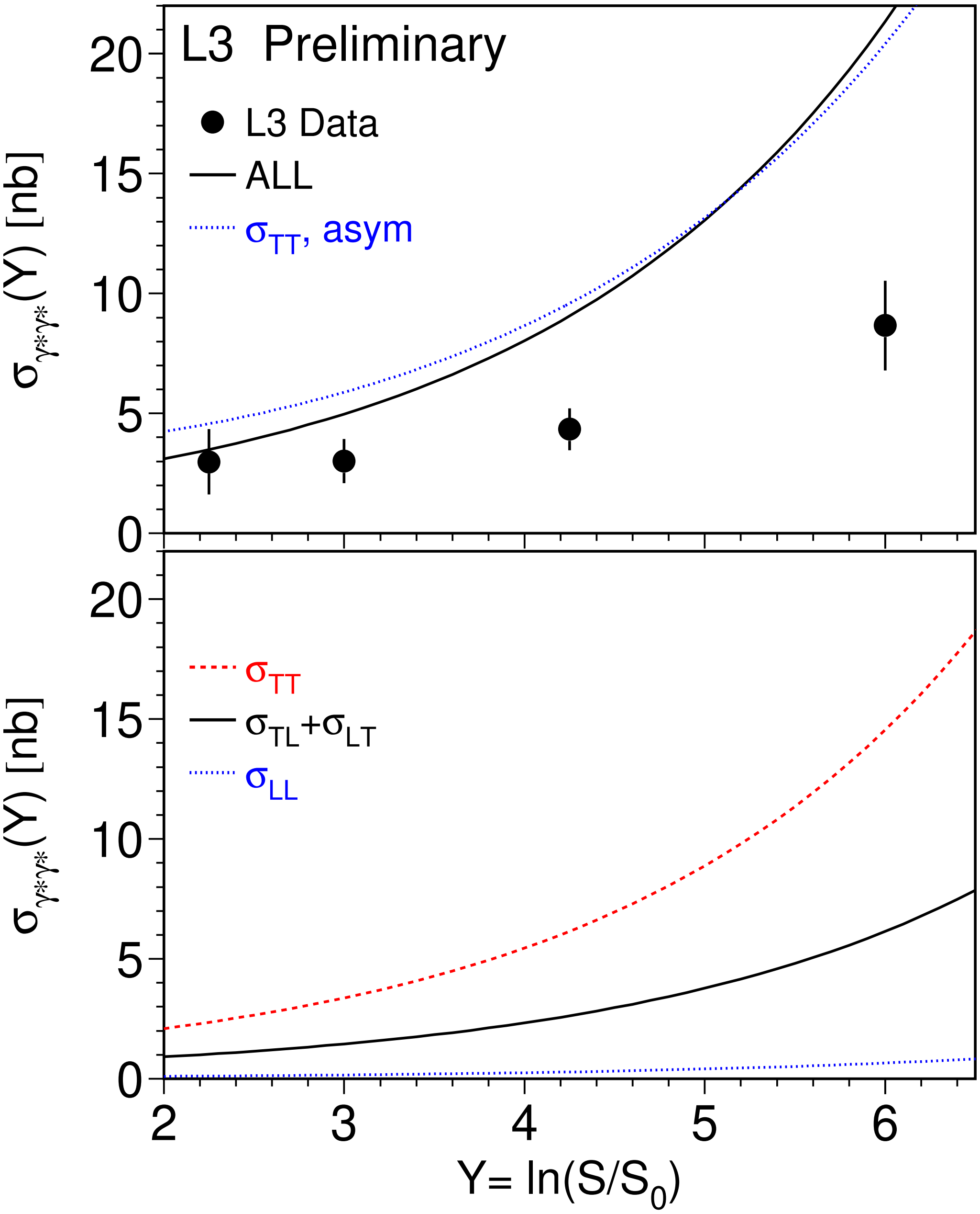

Figure 9: Two-photon cross-sections, $\sigma_{\gamma^*\gamma^*}$ at ($\langle Q^2 \rangle = 15$ GeV^2, $\alpha_s = 0.206$). (top) The exact LO BFKL calculations including the charm mass ($\mathrm{m_c} = 1.5$ GeV), all the photon polarization states and the variation of the strong coupling constant (solid line) and the LO BFKL calculation at the saddle point approximation(dotted line). (bottom) Contribution of the different polarizations to the double-tag cross section.